*Arc Volcanism: Physics and Tectonics*, edited by D. Shimozuru and I. Yokoyama, 95–113.


# A Theoretical Model for Dispersion of Tephra

Takeo SUZUKI

*Department of Physics, The Institute of Vocational Training, Sagamihara, Kanagawa 229, Japan*

The dispersion of tephra is a function of many factors: total mass, median diameter and standard deviation of material erupted, height of the eruption column, wind velocity, and the nature of particle diffusion from the eruption column. The relationship between these factors and the dispersion of tephra is made clear using a model of two-dimensional diffusion in the atmosphere. It was found that the shape of the curves showing the relationship between logarithmic mass per unit area of deposited tephra and logarithmic area enclosed by iso-mass contours is a function of the standard deviation of material erupted; the inflection-point of the curves is a function of median diameter of the material erupted and height of the eruption column. Variations in wind velocity have an effect upon the shape of the dispersion isopleth curves. The effects of total mass of tephra on dispersal patterns may be expressed by plotting the area enclosed by iso-mass contours as a function of mass per unit area. Variations in total mass cause the resulting curves to shift laterally, but do not change their basic shape.

A quantitative definition for the classification of "bigness" by Walker is proposed for comparison of various volcanic eruptions.

## 1. Introduction

The mass of erupted material and the areal extent and thickness of tephra fallout are primary factors in understanding the destructive potential of volcanic eruptions. The former is a function of the total energy of a volcanic eruption, and the latter depends upon the specific expression of this energy; that is, the initial size of ejected tephra, the extent of fragmentation of the tephra, and the height of the eruption column, as well as wind velocity and wind direction. Therefore, tephra fallout patterns may vary greatly in individual eruptions and the tephra takes on a variety of the destruction even though total mass of erupted material may be the same.

The total mass of erupted material is estimated from the accumulation volume of the tephra by empirical methods, since there is no general theoretical basis for computation. The author investigated the relationship between the thickness of air fall deposits and area enclosed by isopach lines and deduced the following formula:

$$Y = A \cdot X^n, \quad X = \log_{10}(h_{max}/h), \quad Y = \log_{10}(S/S_0).$$

$S$: the area enclosed by isopach of thickness $h$. $S_0$: that of maximum thickness $h_{max}$ (SUZUKI, 1981). This curve was called the "thickness-isopach area" curve which does not conflict with the following assumptions:

(a) The erupted material consists of a finite quantity of volcanic particles.
(b) The distribution of the diameter of these particles has a single mode.
(c) All of the particles fall at terminal velocity and finally accumulate on the ground.

Meanwhile, there is no empirical method proposed for the dispersion of tephra, which depends upon many factors and conditions at the time of an eruption. Their effect on the dispersion of tephra must be investigated. The simulation based on the data gathered during volcanic eruptions at present is a better method to determine the factors and the conditions of ancient tephra eruptions.

The data on air-fall deposits obtained in the field and the laboratory are thickness, particle size distribution, proportion of pumice to lithic fragments, bulk density of deposits, and density of particles. All of these data are a function of sampling sites and yield information on the conditions at the time of eruption, total quantity of erupted material and its particle size distribution, height of the eruption column, velocity and direction of wind, vertical velocity within the eruption column, and diffusion of volcanic particles from the eruption column. Interpretation or estimation of these phenomena of volcanic eruptions from the field data of tephra characteristics is a very useful technique for the study of volcanic activity and estimation of volcanic disaster-potential.

Figure 1 shows the relationship of total mass of tephra and its dispersal area to the destructive potential of volcanoes, and indicates observable or measurable characteristics of eruptions that are necessary for understanding the dispersive activity of an eruption column.

TSUYA (1955) classified the intensity of volcanic activity into ten grades, founding on the volume of erupted material. WALKER (1980) pointed out that explosive volcanic eruptions show five kinds of "bigness:" magnitude, intensity, dispersive power, violence, and destructive potential. He defined the magnitude as the total energy released by the eruption, and proposed that the magnitude is expressed by the dense rock equivalent volume (DRE). Alternatively, YOKOYAMA (1956) calculated the thermal energy founding on the total mass of erupted products. The author prefers to define magnitude of volcanic eruptions by means of total mass of eruptive products (see Appendix).

In this paper dispersion of tephra is investigated using a two-dimensional diffusion model. This model is based on the following factors:

(1) Diffusion of volcanic particles from an eruption column.
(2) Horizontal transfer of these particles with the horizontal movement of the atmosphere.
(3) Horizontal diffusion of the particles due to turbulency of the atmosphere.
(4) Sinking of the particles in the atmosphere.

## 2. Dispersion of Tephra in the Atmosphere

Since the movement of air mass is random in time and space due to the interaction of many eddies, movement of dispersing particles in the atmosphere is also random. Small particles diffuse in the atmosphere in both vertical and horizontal directions;

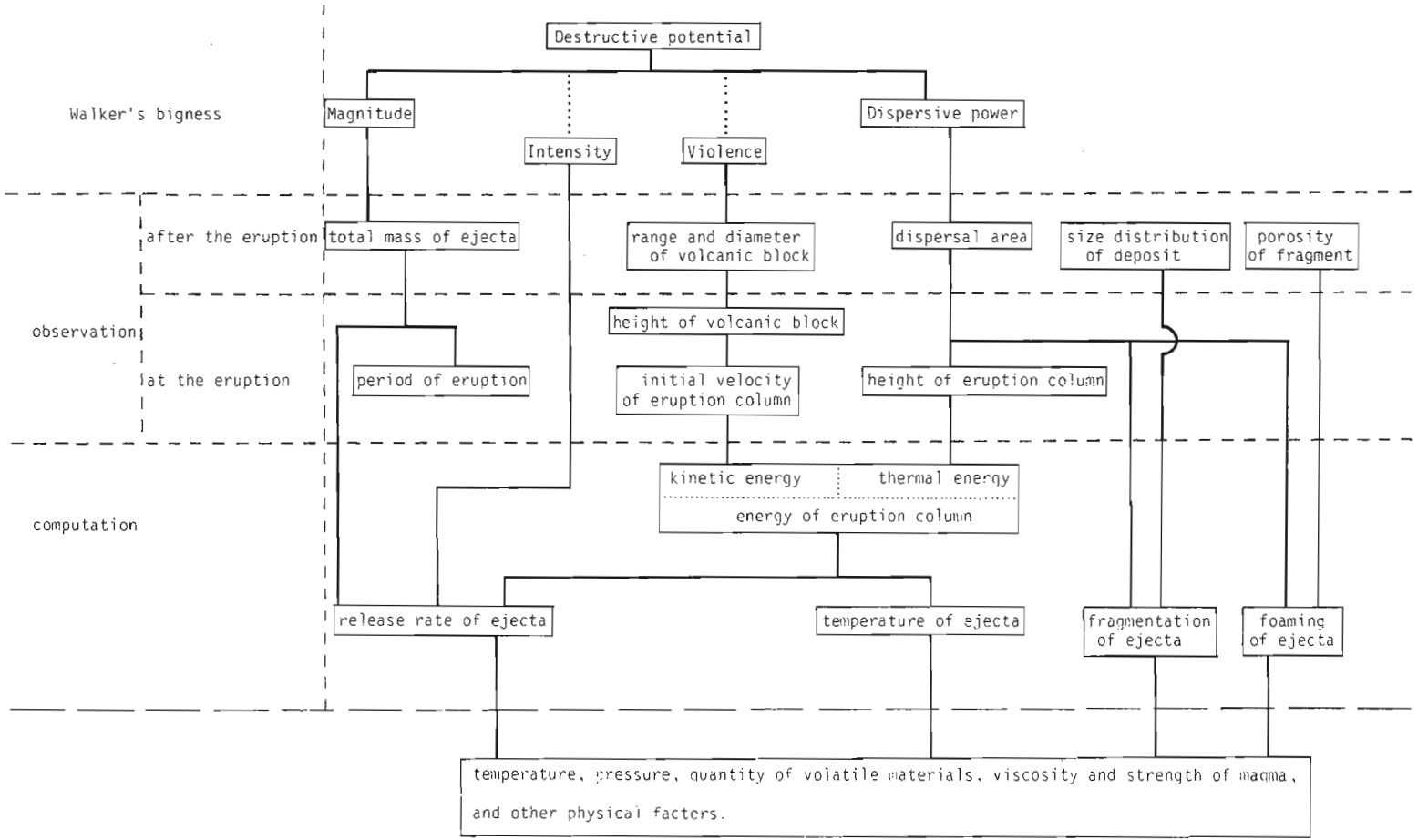


Fig. 1. Block diagram showing the relationship of the factors concerned with volcanic eruptions.

however, the scale of horizontal turbulence is much greater than that of vertical turbulence. In this paper, therefore, particle dispersion is investigated using a two-dimensional diffusion model in which only horizontal turbulent diffusivity is considered.

The two-dimensional differential equation for diffusion in wind of uniform velocity, taking $x$ leeward (CSANADY, 1973), is as follows

$$\frac{\partial \chi}{\partial t} = -u\frac{\partial \chi}{\partial x} + \frac{\partial}{\partial x}\left(K\frac{\partial \chi}{\partial x}\right) + \frac{\partial}{\partial y}\left(K\frac{\partial \chi}{\partial y}\right), \tag{1}$$

where $\chi$ is the concentration of the diffusing substance, $K$ is the eddy diffusivity, and $u$ is the velocity of wind. The eddy diffusivity $K(r, t)$ in turbulent diffusion is a function of the distance $r$ from the center of diffusion and the diffusion time $t$, where $r = \{(x - ut)^2 + y^2\}^{1/2}$.

The function form of $K(r, t)$ has been expressed in various ways. Comparison of the solution of Eq. (1) with published data was made by using the following variance $\sigma_r^2$ and apparent eddy diffusivity $A_L$.

$$\sigma_r^2 \equiv \int_0^\infty r^2 \cdot \chi(t, r) \cdot 2\pi r \, dr \Big/ \int_0^\infty \chi(t, r) \cdot 2\pi r \, dr, \quad A_L \equiv \sigma_r^2/4t.$$

For the typical $K(r, t)$, $\sigma_r^2$ and $A_L$ are as follows:

| | | |
|---|---|---|
| Fick type diffusion | $K = \text{const.}$; | $\sigma_r^2 \propto t$, $A_L = K$ |
| JOSEPH and SENDNER (1958) | $K \propto r$; | $\sigma_r^2 \propto t^2$, $A_L \propto L$ |
| OZMIDOV (1958) | $K \propto r^{4/3}$; | $\sigma_r^2 \propto t^3$, $A_L \propto L^{4/3}$ |

where $L \equiv 3\,\sigma_r$.

On the basis of observations, the following relations have been reported.

| | |
|---|---|
| $A_L \propto L^{4/3}$ | (RICHARDSON, 1926) |
| $\sigma_r^2 \propto t^2 \sim t^3$ | (BATCHELOR, 1950) |
| $A_L \propto L^{1.1}$, $\sigma_r^2 \propto t^{2.3}$ | (OKUBO, 1971) |

The above stated $K$ is expressed as a function of $r$ only. In the turbulent diffusion of air-fall particles, however, the diffusion time is the fall time of particles. The eddy diffusivity $K$ may, therefore, also be a function of the fall time of particles. The scale and time effects of turbulent diffusivity are caused by superposition of the effects of many eddies, and the effect of large-scale eddies may be equivalent to that of plolonged time in the random movements of dispersing particles. The solution of Eq. (1) is obtained by writing $K = C\,t^{3/2}$

$$\chi = \frac{5q}{8\pi C\,t^{5/2}} \exp\left[-\frac{5\{(x - ut)^2 + y^2\}}{8C\,t^{5/2}}\right], \tag{2}$$

where $C$ is a constant and $q$ is the amount of material. Equation (2) gives the variance and the apparent eddy diffusivity as follows:

$$\sigma_r^2 = \left(\frac{8C}{5}\right) t^{5/2}, \quad A_L = 0.08073\, C^{2/5} L^{6/5}.$$

The assumption for $K = Ct^{3/2}$, therefore, satisfies Eq. (1) and is compatible with the observed data of Richardson, Batchelor, and Okubo. The data on diffusion in the atmosphere shown in Fig. 2 gives

$$A_L = 0.887 L^{6/5},$$

where $A_L$ is given in $cm^2/s$ and $L$ in cm, and hence $C = 400$.

## 3. Atmospheric Settling Velocity of Pyroclastic Particles

WALKER *et al.* (1971) determined the terminal fall velocity of pyroclastic particles by laboratory measurements, and calculated the sea-level terminal fall velocity of particles with various sizes and densities. WILSON (1972) estimated the fall time of pyroclastic particles from great height using Walker *et al*'s method. WILSON and HUANG (1979) founding on the laboratory measurement of terminal fall velocities for pumice, glass shards and feldspar crystals of ash size, proposed the following formula on the relationship between the drag coefficient $C_a$, Reynold's number $R_a$ and shape parameter $F$,

$$C_a = \frac{24}{R_a} F^{-0.828} + 2\sqrt{1.07 - F}, \tag{3}$$

where

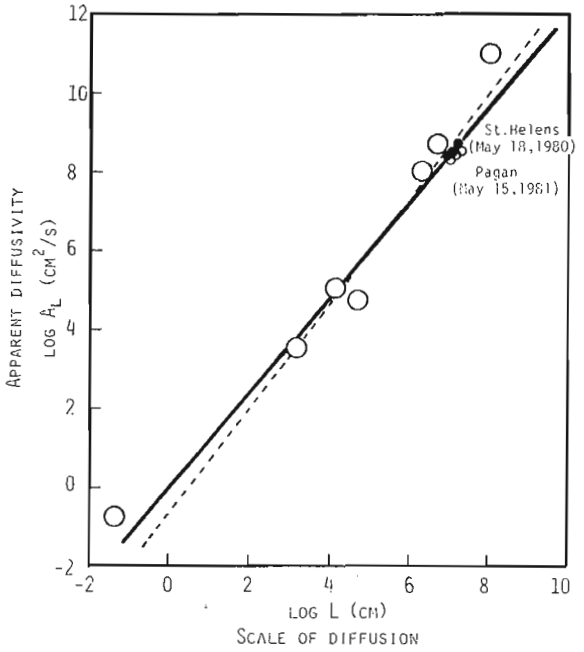


Fig. 2. Diffusion diagram for apparent diffusivity vs. scale of diffusion in the atmosphere. The large open circles and dotted line are from RICHARDSON (1926), the solid line is $A_L = 0.887\ L^{6/5}$.

$$C_a = \frac{4\psi_p g d}{3\psi_a V_t^2},\quad R_a = \frac{\psi_a V_t d}{\eta_a},\quad F = \frac{b+c}{2a},\quad d = \frac{a+b+c}{3}$$

($d$ is the mean diameter of particles with principal axes $a, b, c$ ($a$ is the longest)), $V_t$ is the terminal velocity of the particle, $\eta_a, \psi_a$ are the viscosity and density of air, $\psi_p$ is the density of particles, and $g$ is the acceleration due to gravity.

Equation (3) gives the terminal fall velocity $V_t$ as a function of the mean diameter $d$ and shape parameter $F$ of particles:

$$V_t = \frac{\psi_p g d^2}{9\eta_a F^{-0.828} + \sqrt{81\eta_a^2 F^{-1.656} + \frac{3}{2}\psi_a \psi_p g d^3 \sqrt{1.07 - F}}}. \tag{4}$$

For particles having a mean diameter less than 0.01 cm, however, the terminal fall velocity for pumice estimated by Eq. (4) does not agree with the experimental data obtained by WILSON and HUANG (1979). Equation (3) depends heavily on the data for glass shards. They used 2.40 (g/cm$^3$) for the density of all glass-shards, and ascribed the change of $C_a$ to the shape parameter $F$. However, the assumption of uniform 2.40 (g/cm$^3$) density for glass-shard is questionable, because the effects of density and the shape parameter on $C_a$ cannot be separated. On the basis of experimental measurements of pumice and feldspar crystals, Eq. (3) is corrected as follows:

$$C_a = \frac{24}{R_a} F^{-0.32} + 2\sqrt{1.07 - F}, \tag{3}'$$

and Eq. (4) is corrected to

$$V_t = \frac{\psi_p g d^2}{9\eta_a F^{-0.32} + \sqrt{81\eta_a^2 F^{-0.64} + \frac{3}{2}\psi_a \psi_p d^3 \sqrt{1.07 - F}}}. \tag{4}'$$

Figure 3 shows the experimental data and the results using Eqs. (4) and (4)′ for comparison.

On the other hand, in order to calculate the fall time ($T$) from the high altitude, the above expression (4)′ is inconvenient for the successive integration during the passage of particles. Therefore, let us derive a simple formula to calculate the fall time of particles, assuming that the change of fall velocity depends only on the density of surrounding air. The effect of the density change on $V_t$ is indicated in the following equation for terminal fall velocity:

$$V_t = \left(\frac{mg}{C_a A \psi_a}\right)^{\frac{1}{2}},$$

where $m$ is the mass of particle, $A$ is the effective cross-sectional area, $C_a$ is drag coefficient and $g$ is the acceleration due to gravity; then

$$V_z / V_0 \fallingdotseq (\psi_{a0}/\psi_{az})^{\frac{1}{2}},$$

where $V_0$ and $V_z$ are the terminal fall velocity of particle at sea-level and height $z$, and

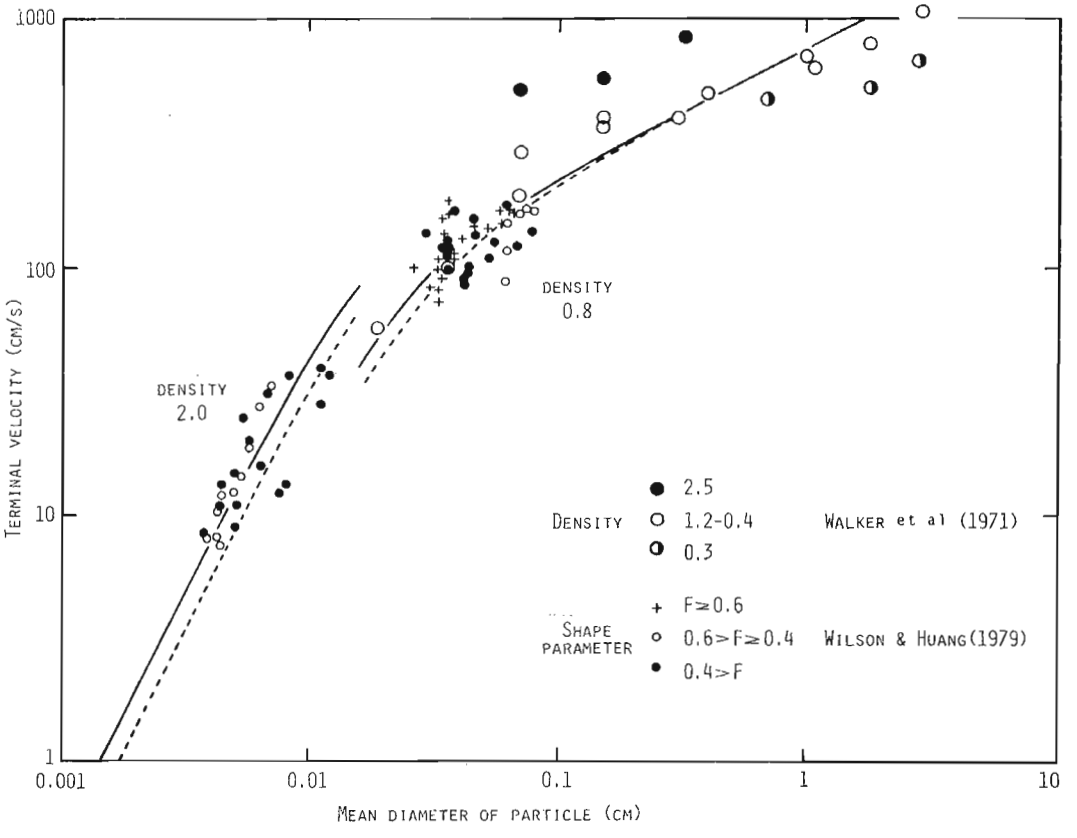


Fig. 3. Terminal fall velocity of volcanic particles vs. mean diameter of the particle at sea-level. Dotted curves; Eq. (4), solid curves; Eq. (4)'. All experimental data are from WALKER *et al.* (1971) and WILSON and HUANG (1979).

$\psi_{a0}$ and $\psi_{az}$ are the density of air at sea-level and height $z$. Assuming constant temperature of air, Boyle's law gives

$$\psi_{az}/\psi_{a0} = \exp\{(-\psi_{a0}/P_0)gz\},$$

where $P_0$ is the atmospheric pressure at sea-level; then

$$V_z = V_0 \exp(0.0625\, z(\text{km}))$$

and the fall time from height $z$ is

$$T = \int_0^z \frac{dz}{V_z} = \frac{1 - \exp(-0.0625\, z(\text{km}))}{0.0625\, V_0}. \tag{5}$$

WILSON (1972) computed the effect of height on the fall time using the Runge-Kutta method for $\eta_a(z)$, $\psi_a(z)$, and $g(z)$. The fall time obtained by Eq. (5) agrees roughly with that of Wilson. Figure 4 shows the fall time deduced from WILSON (1972) compared with that calculated from Eq. (5). In order to reduce the slight disagreement, the following corrections should be done:

$$t = 0.752 \times 10^6 \left[ \frac{1 - \exp(-0.0625z)}{V_0} \right]^{0.926}, \qquad (5)'$$

where $t$ is given in seconds, $z$ in km, and $V_0$ in cm/s. The corrected relation is shown by a solid line in Fig. 4.

## 4. Diffusion of Volcanic Particles from the Eruption Column

The size distribution of erupted pyroclastic material may be explained by Rosin's law, or logarithmic probability distribution. In this paper the latter distribution is adopted. The function of probability density is given by

$$f(\log_{10} d) = \frac{1}{\sqrt{2\pi}\,\sigma_d} \exp\left\{ - \frac{(\log_{10} d/d_m)^2}{2\sigma_d^2} \right\},$$

where $\sigma_d$ is the standard deviation of size distribution and $d_m$ is the median diameter. The quantity $dq$ of particles having diameters between $d_j$ and $d_{j+1}$ for the total quantity of erupted material ($Q$) is

$$dq = \frac{Q \log_{10}\left(\frac{d_{j+1}}{d_j}\right)}{\sqrt{2\pi}\,\sigma_d} \exp\left\{ - \frac{(\log_{10} d_j/d_m)^2}{2\sigma_d^2} \right\}. \qquad (6)$$

Previous study of the diffusion of particles from an eruption column has left the problems of diffusion unsolved. MORTON *et al.* (1956) and others studied the vertical velocity of a thermal plume by theoretical and experimental methods, and SEINO (1969), BLACKBURN *et al.* (1979), and others have studied the vertical velocity of volcanic eruption columns. The theories are complicated and results differ from each other.

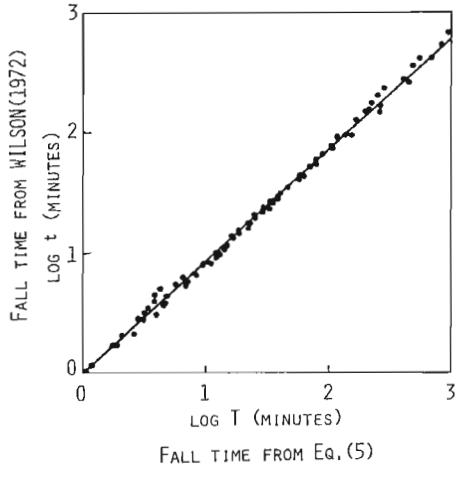


Fig. 4. Comparison of tephra fall times deduced from WILSON (1972) and from Eq. (5). Solid line is $t = T^{0.926}$.

In this paper, therefore, a convenient model in which the vertical velocity of a volcanic eruption column is maximum at the vent and zero at the top of the column is adopted, and the diffusion of volcanic particles from an eruption column is calculated on the following assumptions:

(1) The vertical velocity of a volcanic eruption column $W(z)$ is a function of height $z$.

$$W(z) = W_0\left(1 - \frac{z}{H}\right)^{\lambda},$$

where $W_0$ is the initial velocity at $z = 0$, $H$ is the maximum height of the eruption column, and $\lambda$ is a constant.

(2) The diffusion parameter of the eruption column $Y$ is a function of the vertical velocity of column $W(z)$ and the terminal fall velocity of particle at sea-level $V_0$ as follows:

$$Y(z) = \frac{\beta\{W(z) - V_0\}}{V_0},$$

where $\beta$ is a constant.

(3) The probability density of diffusion $P(z)$ is a function of parameter $Y$ as given by the equation

$$P(z) = A\,Y\exp(-Y),$$

where $A$ is given by

$$\int_0^H P(z)\mathrm{d}z = 1.$$

Under these assumptions, we get the probability density of diffusion $P(z)$ for $\lambda = 1$ as follows:

$$P(z) = \frac{\beta W_0 Y \exp(-Y)}{V_0 H\{1 - (1 + Y_0)\exp(-Y_0)\}}, \tag{7}$$

where

$$Y_0 = \beta(W_0 - V_0)/V_0.$$

The eruption column is fan-shaped upwards; the diffusion source is generally not a point source. The radius of the eruption column is assumed to be $0.5\,z$, where $z$ is the height, and is equal to three times the standard deviation $\sigma_r$; hence $3\,\sigma_r = 0.5\,z$. From Eq. (2) the variance $\sigma_r^2 = (8/5)Ct^{5/2}$ and the time $t_s$ for $\sigma_r = 0.5\,z/3$ is given as follows:

$$t_s = \left(\frac{5z^2}{288C}\right)^{2/5}.$$

This $t_s$ is added only to the diffusion time in Eq. (2), and not to the horizontal transfer time.

## 5. The Total Mass of Erupted Material and Its Aerial Distribution

The quantity $dq$ of particles having diameters between $d_j$ and $d_{j+1}$ is given by Eq. (6). The quantity $q(d, z)$ of the particles diffused at height $z \sim z + dz$ is

$$q(d, z) = dq\, P(z)\, dz.$$

By substituting $q$ into Eq. (2), the quantity of accumulation at the point $(x, y)$on the earth's surface, when $\chi$ in Eq. (2) is integrated over all sizes of particles and all heights of the eruption column, is given as follows:

$$X(x,y) = \int_{d=0}^{d=\infty} \int_0^H \frac{5P(z)}{8\pi C t^{5/2}} \exp\left[ -\frac{5\{(x-ut)^2 + y^2\}}{8Ct^{5/2}} \right] dq\, dz. \tag{8}$$

The diffusion time $t$ is given by Eq. (5)′, and $V_0$ in Eq. (5)′ is given by Eq. (4)′ as a function of the diameter of particles $d$.

## 6. Results of Numerical Computation

On the basis of the previous arguments, we shall simulate the dispersion of tephra from the eruption column. The quantity $Q = 10^{15}$ gram is used in the present computation for the total quantity of erupted material, This quantity is nearly equal to 1 km$^3$ of tephra. As shown in Eq. (6), the quantity of accumulation at any point on the surface is proportional to the total quantity of erupted material, if other parameters are constant, as is obvious from Eq. (6) and Eq. (8).

The range of values used in the present computation is 0.01–10 cm for median diameter $d_m$, 0.1–2.0 for the standard deviation of size distribution $\sigma_d$, 3–30 km for the height of eruption column $H$. For the simplicity, the horizontal wind velocity is constant through the concerned altitude, which is assumed to be 5–30 m/s.

A typical size distribution of erupted material is shown in Fig. 5. The particle diffusion from the eruption column is almost controlled by the value of $\beta W_0$ in Eq. (7). The mass diffusion from the eruption column as a function of $\beta$ is shown in Fig. 6(a), where $10^4$ cm/s is used for the value of $W_0$ (initial velocity in the eruption column); 0.1 cm is used for $d_m$, 0.4 for $\sigma_d$ and 10 km for $H$. Fig. 6(b) shows iso-mass distribution maps and Fig. 6(c) shows variations of mass per unit area on the axis of mass distribution as a function of distance from the vent. In the case of large $\beta$, mass diffusion takes place in the upper part of the eruption column as shown in Fig. 6(a) and the distribution has a maximum mass per unit area at some distance from the vent (Fig. 6(b), $\beta = 0.5$). Such bimodal tephra distribution is reported in some cases, but quite seldom. The value of $\beta$ takes, therefore, 0.1, and hence, $\beta W_0 = 10^3$ cm/s.

For $\beta = 0.1$ in Fig. 6(a), the variation of the mass diffusion from the eruption column with $d_m$, $\sigma_d$, and $H$ is shown in Fig. 7(A), (B), and (C), respectively. In these figures, $f$, $m$, and $c$ show fine, medium, and coarse particle, respectively. Figure 8 shows the distribution area enclosed by the 10 gram per unit area estimated by using Fig. 7. Figures 8(A), (B), and (C) correspond to Figs. 7(A), (B), and (C) for $u = 10$ m/s, respectively. Figure 8(D) shows the variation of the distribution area with $u$ for $\beta = 0.1$ in Fig. 6(a). Figure 9 shows the variation of mass per unit area on the mass distribution

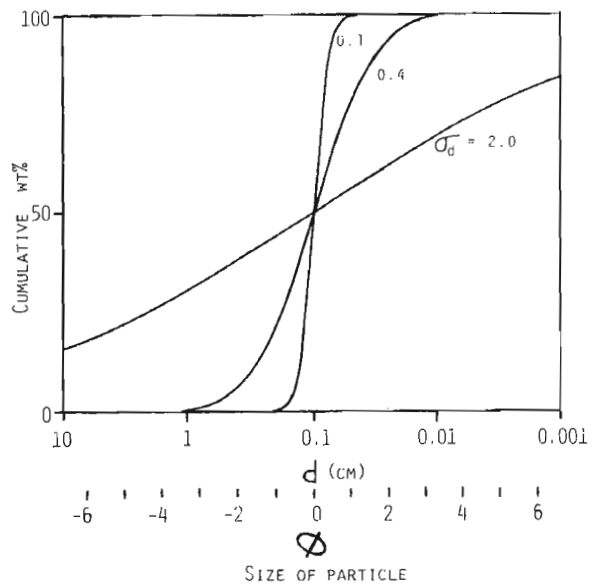


Fig. 5. Size-distribution of material erupted. Median diameter $d_m = 0.1$ cm and standard deviation $\sigma_d = 0.1$, 0.4, and 2.0.

axis with distance from the vent shown in Fig. 8, and Fig. 10 shows the variation of the area enclosed by isopleths of mass per unit area, the area enclosed by iso-mass contours, with the mass per unit area.

For tephra having small median diameter, mass diffusion takes place in the upper part of eruption column, as shown in Fig. 7(A) (a), and the dispersion area is broad at a distance, as shown in Fig. 8(A). The accumulated mass is small near the vent and is commonly maximum at a distance, as shown in Fig. 9(A). The iso-mass lines enclose a large area of thin tephra accumulation, as shown in Fig. 10(A). For large median diameter, on the other hand, mass diffusion takes place in the lower part of the eruption column. The dispersion area is a small oval near the vent, and the accumulated mass is greatest near the vent. The area enclosed by iso-mass lines is small and the ash accumulation thick.

Variation of $\sigma_d$ has a remarkable effect on the mass diffusion, as shown in Fig. 7(B). The shape of the dispersion area is an oval lying inside the vent for large, $\sigma_d$, and is spread in a fan-shape from the vent for small $\sigma_d$, as shown in Fig. 8(B). The accumulated mass decreases linearly with distance for large $\sigma_d$, decreases sharply at a distance with the decrease of $\sigma_d$ and is maximum at a distance for small $\sigma_d$, as shown in Fig. 9(B). The area enclosed by iso-mass lines decreases linearly with increasing mass per unit area for large $\sigma_d$, but for small $\sigma_d$, it remains almost constant at a certain value of the mass per unit area and then decreases sharply, as shown in Fig. 10(B).

As to the relationships between mass diffusion and height (Fig. 7(C)), the shape of the dispersion area (Fig. 8(C)), the accumulated mass (Fig. 9(C)), and the area enclosed by iso-mass (Fig. 10(C)), each of them has similar shapes for the variation of the height

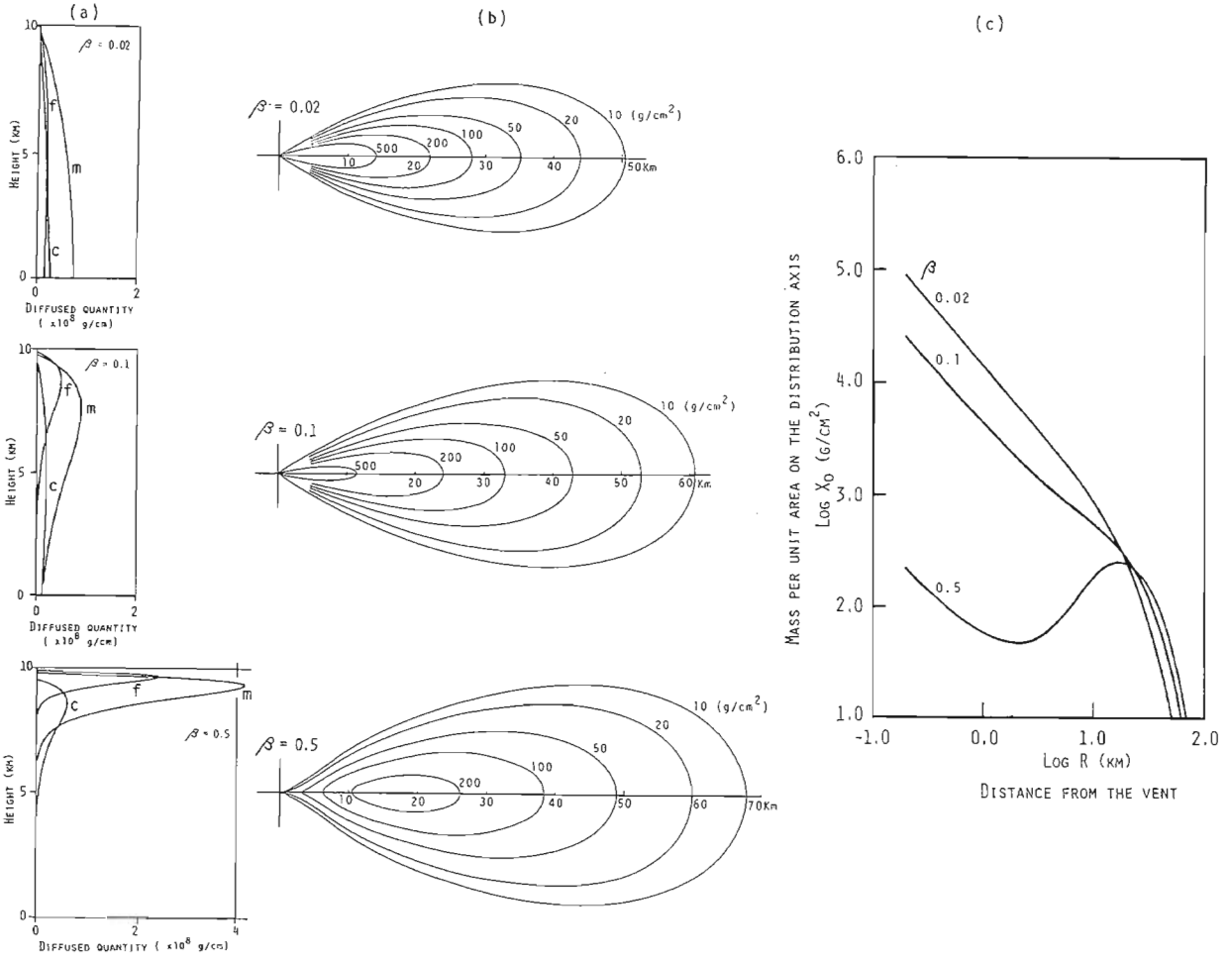


Fig. 6. Dispersion vs. $\beta W_0$. $Q = 10^{15}$ gram, $W_0 = 10^4$ cm/s, $d_m = 0.1$ cm, $\sigma_d = 0.4$. $H = 10$ km, and $u = 10$ m/s in three values of $\beta$. (a): Mass of material diffused per unit height vs. height in an eruption column. (b): Iso-mass maps (maps of isopleths of mass in gram/cm$^2$). (c): Variation of mass per unit area on the distribution axis with distance from the vent.

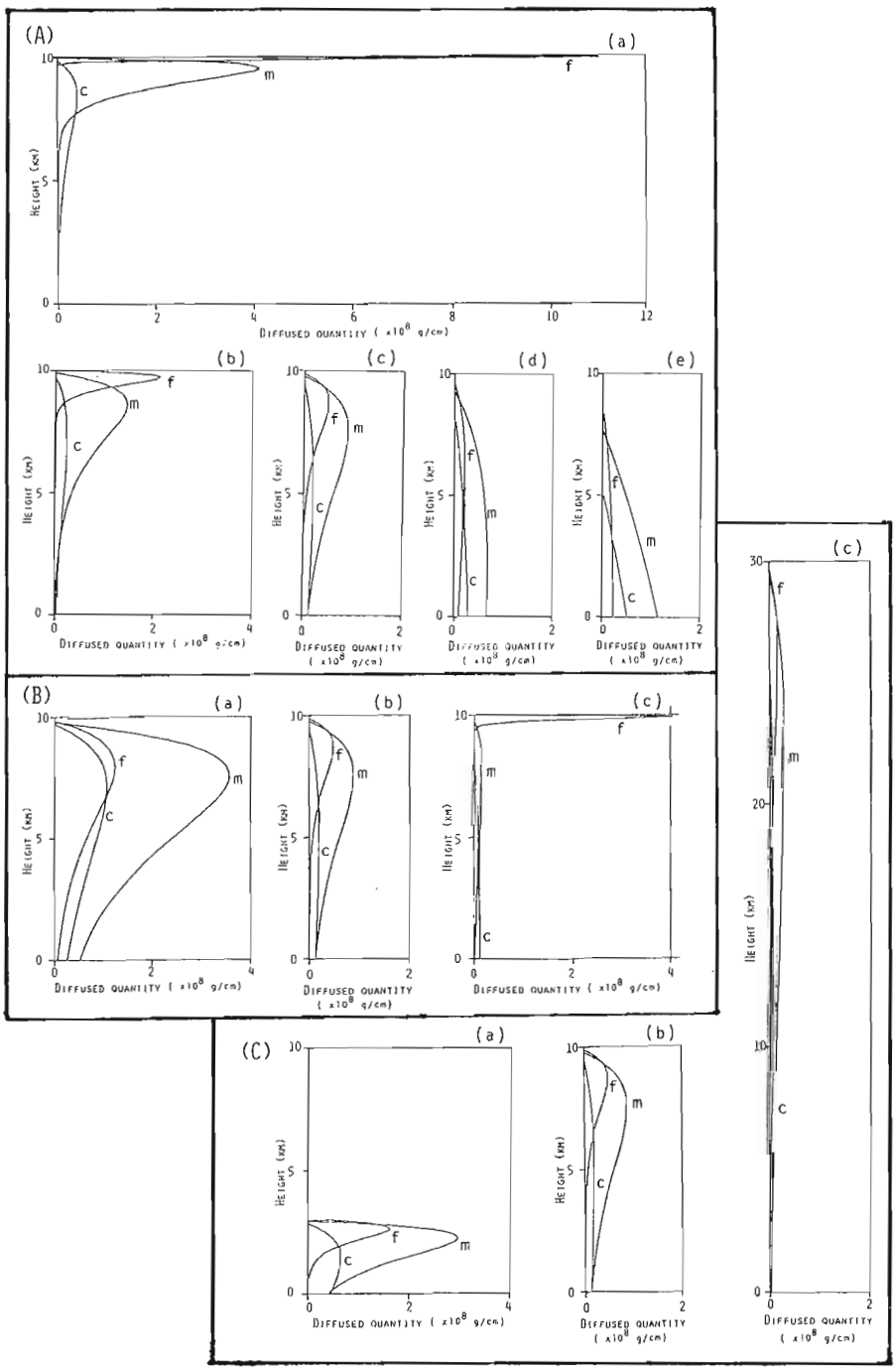


Fig. 7. Mass of material diffused per unit height vs. height in an eruption column. (A): (a) $d_m = 0.01$ cm, (b) $d_m = 0.03$ cm, (c) $d_m = 0.1$ cm, (d) $d_m = 1$ cm, (e) $d_m = 10$ cm; $\beta W_0 = 10^3$ cm/s, $\sigma_d = 0.4$, $H = 10$ km, (B): (a) $\sigma_d = 0.1$, (b) $\sigma_d = 0.4$, (c) $\sigma_d = 2.0$; $\beta W_0 = 10^3$ cm/s, $d_m = 0.1$ cm, $H = 10$ km. (C): (a) $H = 3$ km, (b) $H = 10$ km, (c) $H = 30$ km; $\beta W_0 = 10^3$ cm/s, $d_m = 0.1$ cm, $\sigma_d = 0.4$. $f$ : fine size particles. $m$: medium size particles ($=d_m$). $c$: coarse size particles.

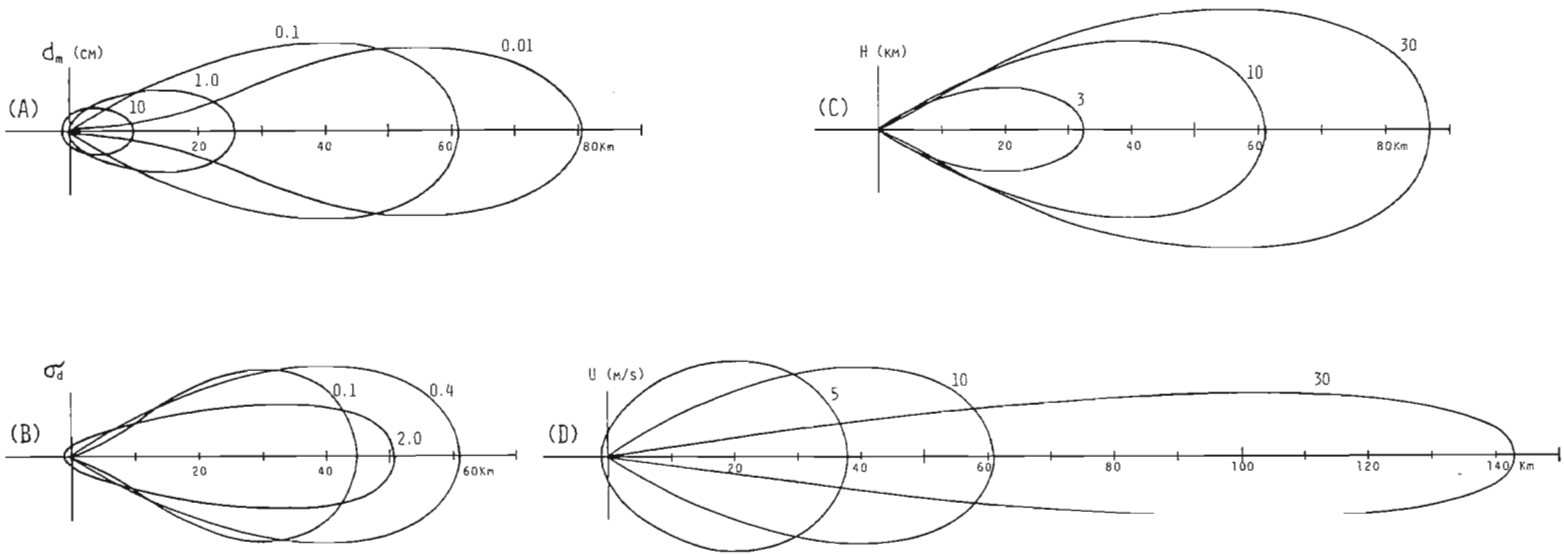


Fig. 8. Area enclosed by isopleths of 10 gram/cm$^2$ for $Q = 10^{15}$ grams. The parameters are chosen as follows: (A) mediam diameter of material erupted; (B) standard deviation of material erupted; (C) height of eruption column; and (D) velocity of wind.

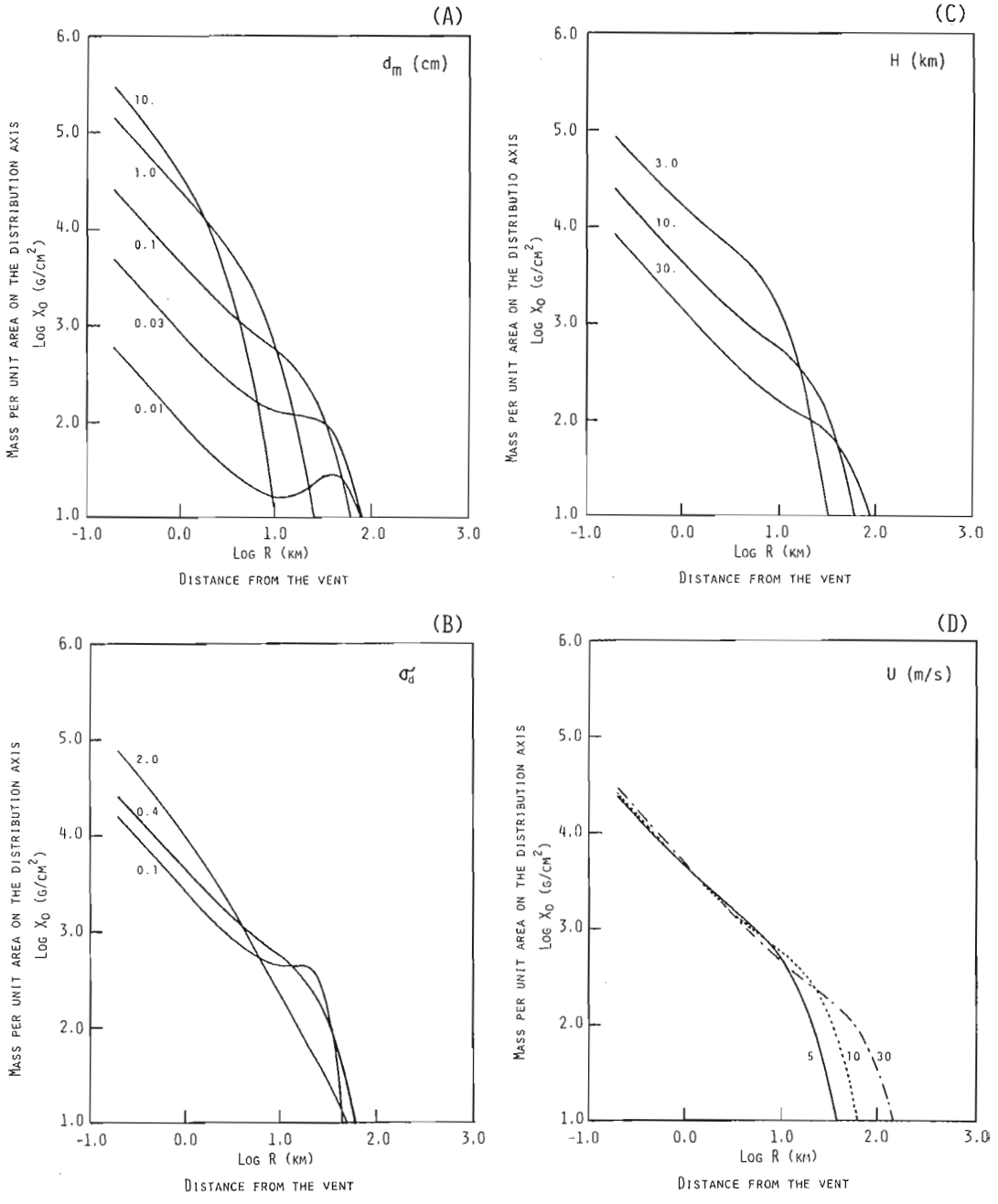


Fig. 9. Variation of mass per unit area on the distribution axis with distance from the vent. The parameters are shown in the top right-hand corner: (A) median diameter of material erupted; (B) standard deviation of material erupted; (C) height of eruption column; and (D) velocity of wind.

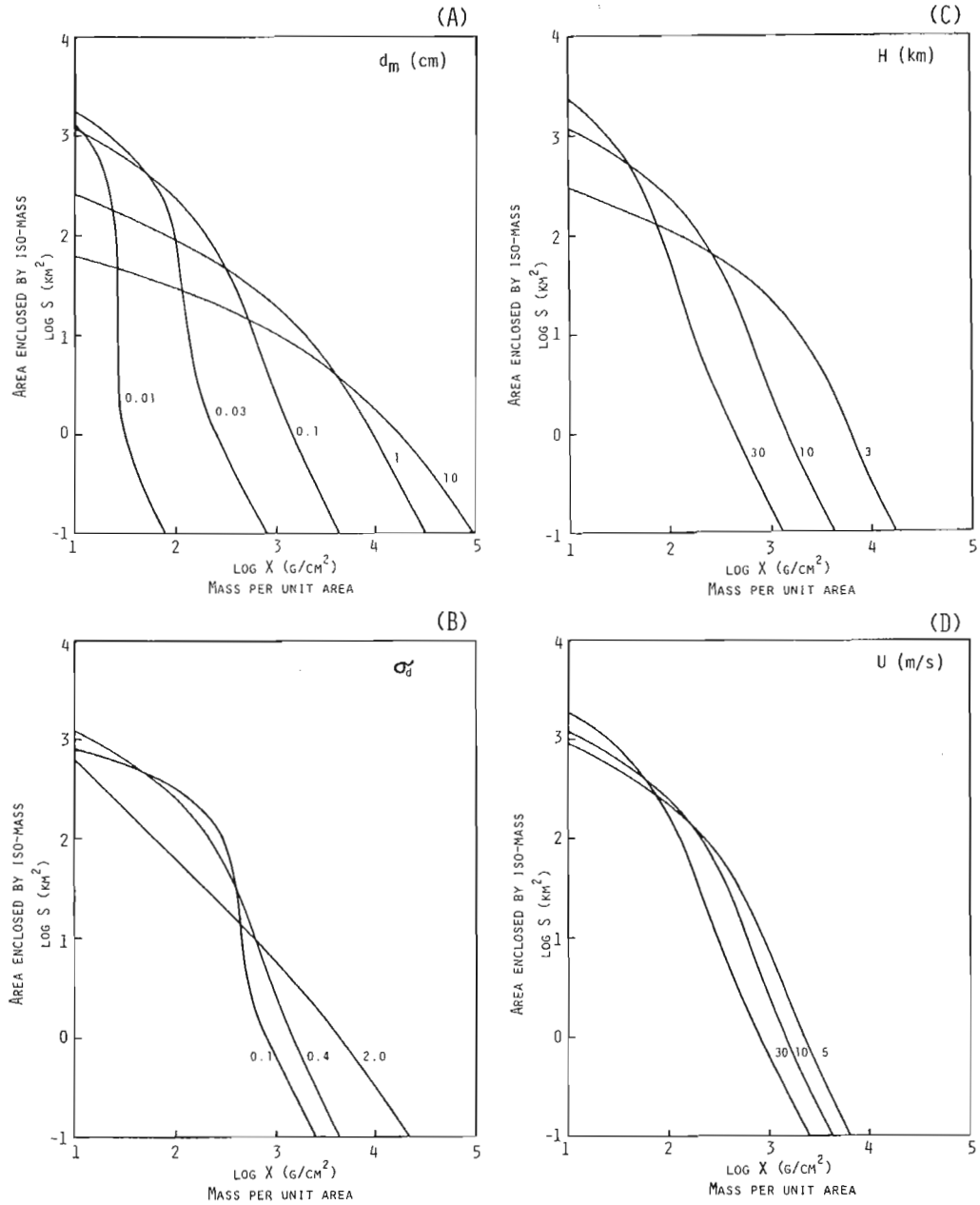


Fig. 10. Mass per unit area vs. area enclosed by isopleths of mass per unit area. The parameters are shown in the top right-hand corner: (A) median diameter of material erupted; (B) standard deviation of material erupted; (C) height of eruption column; and (D) velocity of wind.

of eruption column, if other parameters are constant. The higher the eruption column, the larger the dispersion area is and the less the accumulated mass near the vent.

The dispersion area surrounding the vent is oval for low wind velocity and is elongated leeward for large wind velocity, as shown in Fig. 8(D). In the area near the vent, the accumulated mass decreases outward at an almost constant rate, and the distance from the vent where the mass decreases sharply depends on the wind velocity as shown in Fig. 9(D). The effect of the wind velocity on the area enclosed by iso-mass lines is small, as shown in Fig. 10(D).

## 7. Conclusions

The results of numerical and graphical analysis of tephra diffusion and dispersion in the atmosphere lead to the following conclusions:

(1) The variations in the total mass of tephra do not affect the dispersal pattern, and the mass per unit area in the dispersion area is in proportion to the total mass.

(2) For an eruption column with ejecta of large median diameter and at low wind velocity, the iso-mass contour lines of tephra accumulation are almost a circle with the center located at the eruptive vent.

(3) For a high eruption column with ejecta of small median diameter and small standard deviation of size distribution, the dispersion area is the broadest and has a maximum mass per unit area at some distance from the vent.

(4) For an eruption column with large median diameter and large standard deviation of material erupted, the tephra dispersion curves show that the mass per unit area of tephra decreases at a logarithmically linear rate with increasing distance from the vent, and the area enclosed by iso-mass contours decreases almost logarithmic-linearly with increasing mass per unit area.

Comparison of the results of computational model studies of tephra dispersion with the dispersion pattern of tephra in the field, based on observation of actual eruption columns, will help clarify the mechanisms of ash diffusion from eruption columns. There are many aspects of volcanic eruptions and characteristics of eruption products that can be studied by empirical methods to shed additional light on these mechanisms. Study of total mass of tephra and dispersion patterns of the material erupted, lithic fragment-pumice ratios, porosity of pumice, and others will accelerate analysis of the dynamic mechanisms of volcanic eruptions.

The author will discuss the relationship between the size distribution of tephra deposits and the factors of the dispersion in later papers, using this model of tephra dispersion.

The author wishes to thank Prof. Tsutomu Murase of our institute for his valuable advice and encouragement.

## APPENDIX

The classification of "bigness" by WALKER (1980) is very useful for the investigation of the relationships between the destructive potential of volcanoes and

these factors. His classification, however, is qualitative and a quantitative definition of "bigness" is necessary for more rigorous analysis of volcanic eruptions. A quantitative definition of "bigness" is proposed as follows:

(1) Magnitude, $M_g$

"Magnitude" is defined by the total mass of erupted material, because the total energy of a volcanic eruption is calculated from the total erupted mass:

$$M_g = \log_{10} M \,(\mathrm{kg}),$$

where $M$ is total mass of ejecta. If the erupted material is all essential material, the total energy of a volcanic eruption is given by $\log_{10} E\,(\mathrm{J}) = 6.2 + M_g$, where J is Joule, (NAKAMURA, 1965).

(2) Intensity, $I_t$

"Intensity" is defined by the mass emission rate.

$$I_t = \log_{10} \dot{M} \,(\mathrm{kg/s}),$$

where $\dot{M}$ is the mass emission rate; $M = \int_0^T \dot{M}\, \mathrm{d}t$, and $T$ is the duration of eruption. The energy emission rate, therefore, is $\log_{10} \dot{E}\,(\mathrm{J/s}) = 6.2 + I_t$.

(3) Dispersive power, $D_p$

"Dispersive power" is defined by the characteristic area of tephra dispersal. This area was discussed by SUZUKI (1981) and is a function not of total mass erupted, but of the height of the eruption column and fragmentation of ejecta:

$$D_p = \log_{10} S_c \,(\mathrm{m}^2),$$

where $S_c$ is defined by the area at the inflection point of the "thickness-isopach area" curve of tephra.

(4) Violence, $V_l$

"Violence" is defined by the vacuum range (WILSON, 1972), because the real range of an ejected volcanic block is a function of the size and density of block. The vacuum range is related to the vertical velocity of the eruption column at the vent.

$$V_l = \log_{10} L_v \,(\mathrm{m}),$$

where $L_v$ is the range in the vacuum expressed in meter.

(5) Destructive potential, $D_t$

"Destructive potential" is defined by the area enclosed by the 10 cm isopach of tephra, because the crops on farm-land are completely destroyed by the air-fall deposit 10 cm thick.

$$D_t = \log_{10} S_{10\,\mathrm{cm}} \,(\mathrm{m}^2),$$

where $S_{10\,\mathrm{cm}}$ is the area enclosed by 10 cm isopach of tephra.

## REFERENCES

BATCHELOR, G. K., The application of the similarity theory of turbulence to atmospheric diffusion, *Quart. J. R. Met. Soc.*, **76**, 133–146, 1950.

BLACKBURN, E. A., L. WILSON, and R. S. J. SPARKS, Mechanisms and dynamics of strombolian activity, *J. Geol. Soc. London*, **132**, 429–440, 1976.

CSANADY, G. T., *Turbulent Diffusion in the Environment*, D. Reidel Publishing Co., Boston, 1973.

JOSEPH, J. and H. SENDNER, Über die horizontale Diffusion im Meere, *Dt. Hydrogr. Z.*, **11**, 49–77, 1958.

MORTON, B. R., Sir G. TAYLOR, and J. S. TURNER, Turbulent gravitational convection from maintained and instantaneous sources, *Proc. R. Soc. London*, A, **234**, 1–23, 1956.

NAKAMURA, K., Energies dissipated with volcanic activities-classification and evaluation, *Bull. Volcanol. Soc. Japan*, **10**, 81–90, 1965.

OKUBO, A., Oceanic diffusion diagrams, *Deep-Sea Research*, **18**, 789–802, 1971.

OZMIDOV, R. V., On the calculation of horizontal turbulent diffusion of the pollutant patches in the sea, *Doklady Akad. Nauk, SSSR*, **120**, 761–763, 1958.

RICHARDSON, L. F., Atmospheric diffusion shown on a distance-neighbour graph, *Proc. R. Soc., London*, A, **110**, 709–737, 1926.

SEINO, M., Motion of volcanic smoke (1), *Bull. Volcanol. Soc. Japan*, **14**, 111–126, 1969.

SUZUKI, T., "Thickness-isopach area" curve of tephra, *Bull. Volcanol. Soc. Japan*, **26**, 9–23, 1981.

TSUYA, H., Geological and petrological studies of volcano, Fuji, 5. On the 1707 eruption of volcano Fuji, *Bull. Earthq. Res. Inst., Univ. Tokyo*, **33**, 341–384, 1955.

WALKER, G. P. L., The Taupo pumice: product of the most powerful known (ultraplinian) eruption? *J. Volcanol. Geotherm. Res.*, **8**, 69–94, 1980.

WALKER, G. P. L., L. WILSON, and E. L. G. BOWELL, Explosive volcanic eruptions-1. The rate of fall of pyroclasts, *Geophys. J. R. Astron. Soc.*, **22**, 377–383, 1971.

WILSON, L., Explosive volcanic eruptions-2. The atmospheric trajectories of pyroclasts, *Geophys. J. R. Astron. Soc.*, **30**, 381–392, 1972.

WILSON, L. and T. C. HUANG, The influence of shape on the atmospheric settling velocity of volcanic ash particles, *Earth* Planet. Sci. Lett., **44**, 311–324, 1979.

YOKOYAMA, I., Energetics in active volcanoes. 2nd paper, *Bull. Earthq. Res. Inst., Univ. Tokyo*, **34**, 75–97, 1956.